Geosynthetics: Leading the Way to a Resilient Planet – Biondi et al (eds)

Predicted performance of geogrid-stabilized unbound aggregate layers using confined soil-geosynthetic composite stiffness

S. Subramanian & J.G. Zornberg
University of Texas at Austin, USA

ABSTRACT: Selection of geosynthetics, for stabilization of unbound aggregate layers in pavements, involves the unconfined properties of geosynthetics and/or the large displacement confined properties. However, geogrids within a pavement system are neither unconfined nor undergo large displacements. This study proposes using the confined Soil-Geosynthetic composite stiffness (K_{SGC}), obtained from Soil-Geosynthetic interaction (SGI) tests, to predict pavement performance when using geogrid-stabilized road bases. A series of identical one-third scale accelerated pavement tests (APTs) were performed on pavement test sections stabilized with various geogrids, diverse in terms of geometry and materials. The rutting from these sections was compared to that in the non-stabilized (control) section to evaluate the Traffic Benefit Ratio (TBR) at failure rut depth for each geogrid. The TBR obtained showed a strong linear correlation to the soil-geosynthetic composite stiffness (K_{SGC}) of the corresponding geogrid obtained from the SGI tests. It is concluded that K_{SGC} is a particularly good indicator of the performance of pavements with geosynthetic-stabilized road bases.

1 INTRODUCTION

Stabilization of unbound pavement layers involves the inclusion of geosynthetics within an unbound aggregate layer and/or at the interface between layers. This is aimed at improving pavement performance by increasing the aggregate layer stiffness through transfer of stresses to the geosynthetic material. In paved roads, this transfer of stresses, to tension-bearing geosynthetic materials, limits the lateral movement of the stabilized pavement layer. This "lateral restraint", which can be mobilized under relatively small deformations, is considered the dominant mechanism of performance improvement for geosynthetic-stabilized paved roads.

Engineering projects specify for geosynthetics based on their index properties such as tensile strength & stiffness, and their performance properties that govern their interaction with surrounding soils such as pull-out resistance or interface shear strength (Zornberg and Christopher (2007)). While these properties are particularly relevant in many engineering applications such as earth-retaining walls, embankments, or slope stability, they are not well suited for the design of stabilized road bases. These properties capture either the small-strain, unconfined behavior (as in the case of tensile stiffness or flexural rigidity) or the large-displacement confined interaction of the geosynthetics with the surrounding soil. However, under serviceable limits for surface pavement, the geosynthetic is under confined conditions but does not undergo large displacements. AASHTO-R50 (2009) recommends performing full-scale tests with geosynthetics to predict their field performance. Some researchers have also developed correlations between geosynthetic properties and their field performance in stabilization (Christopher *et al.* (2008), Archer & Wayne (2012)). However, these correlations lack a mechanistic basis since they are based on properties that do not capture the geosynthetic behavior under serviceable limits for surfaced pavements. In this study, the soil-geosynthetic composite stiffness (K_{SGC}), that captures

DOI: 10.1201/9781003386889-286

the confined small-strain interaction of geosynthetic with soil, is proposed to predict the stabilized pavement performance.

2 ACCELERATED PAVEMENT TEST

In order to access the performance of pavement sections with stabilized base course, reduced-scale pavement sections were constructed in the laboratory under controlled environmental conditions. These sections comprised of identical pavement configuration but with four different types of geogrids (GG1 to GG4 – Figure 1), different in their material and geometric properties (Table 1). One section without any stabilizing geosynthetic was also constructed to serve as the control. All 5 pavement sections consisted of a 15 cm clean uniform sand subgrade placed at 67% relative density, 12.5 cm gravel base conforming to AASHTO#8 gradation and placed at 85% relative density, and 2.5 cm hot mix asphalt (HMA) ride surface from a thin overlay mix – type A (TxDOT SS3239 (2004)). The entire structure was built above grade in two modular frames, each 15 cm tall. The pavement structure was 180 cm (72″) in length and 180 cm in width with a total depth of 30 cm as shown in Figure 2. The geogrid in stabilized sections was placed at 7.5 cm below the HMA surface within the base.

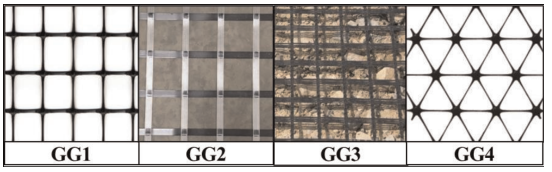

Figure 1. Geogrids used in the SGI test and for stabilization of base course in APTs.

Table 1. Index properties specified by the manufacturers of the geogrids.

Property	GG1	GG2	GG3	GG4
Polymer Type	PP	PP	PP	PP
Manufacturing Process	Punched Drawn	Welded Strips	Woven Yarns	Punched Drawn
Aperture Shape	Rect.	Rect.	Rect.	Triangle
Aperture Dimensions (mm)	33 x 25	41 x 41	15 x 15	33
Rib Width (mm)	3.2	9.0	–	1.0
Minimum Rib Thickness (mm)	0.76	0.6	–	2.0
Tensile Strength @ 1% Strain (kN/m)	–	5.2	–	–
Tensile Strength @ 2% Strain (kN/m)	6.6	8.2	7	–
Tensile Strength @ 5% Strain (kN/m)	13.4	15.1	14	–
Ultimate Tensile Strength (kN/m)	19.0	24.2	23.3	–
Junction Efficiency (%)	93	–	–	93

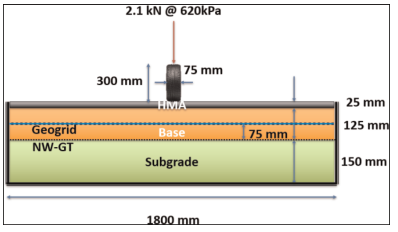

Figure 2. Cross-section of the pavement test section.

Accelerated pavement tests (APTs) were conducted on all 5 sections using the model mobile load simulator (MLS11 – Figure 3) by applying repeated, unidirectional, rolling-wheel loads of 2.1 kN at 620 kPa tire pressure. The pavement structure was subjected to 7200 load repetitions per hour. Additional details about the loading equipment and its capabilities can be found in previous studies such as Epps Martin *et al.* (2003).

A laser distance meter (LDM), attached to the carriage on an actuator, was used to profile the

Figure 3. Model Mobile Load Simulator (MLS11) trafficking the pavement test section.

surface deformations as shown in Figure 4. By controlling the LDM sampling rate and actuator velocity, the vertical distance from the actuator to the pavement surface was captured every 5 mm of horizontal actuator displacement. This allowed for the generation of transverse surface profiles with 360 sample points. The pavement was painted white, at the locations of profiling, in order to improve the reflectivity of the laser. The surface profiles post-trafficking is compared to the initial surface profile to determine rutting at any given number of passes.

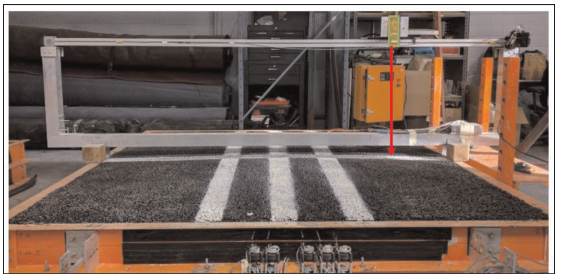

Figure 4. Profilometer mounted on the section (Highlighted in green is the laser distance meter).

3 SOIL-GEOSYNTHETIC INTERACTION TEST

The Soil-Geosynthetic Interaction (SGI) tests is a novel variation of a conventional pull-out resistance test that involves the measurement of internal nodal displacements of the geosynthetic in addition to the external pull-out load and the corresponding frontal displacement of the geosynthetic (Roodi & Zornberg 2017). The SGI tests, performed for this study, involved sandwiching each of the four geogrids (GG1 to GG4) with the clean AASHTO#8 gravel base material, used in the APTs, at 21 kPa confining pressure, and pulling them out as their internal nodal displacements under the applied tensile load were measured. A total of 5 tests were conducted for each geogrid and three nodal displacements were measured per test. Thus, the soil-geosynthetic composite stiffness (K_{SGC}) was calculated as the slope of the square of the unit tension (in (kN)/m) at each node vs. nodal displacement (in mm) of the corresponding node. The K_{SGC} of each geogrid was taken as the

mean of the 15 K_{SGC} values determined as discussed above. In their theoretical formulation of K_{SGC}, Zornberg *et al.* (2017) showed that this slope of the unit tension squared at the node vs. nodal displacement is the same as,

$$K_{SGC} = 4 \cdot J_c \cdot \tau_y \tag{1}$$

where J_C = confined stiffness of the geogrid; and τ_y = yield shear strength.

Therefore, K_{SGC} of the geogrid is a measure that combines the in-isolation stiffness of the geogrid under confined conditions with the interaction of the geogrid with the surrounding soil. A high K_{SGC} indicates that the geosynthetic under consideration is not only stiff but is also capable of significant stress transfer between the soil and the geosynthetic. This implies that K_{SGC} is particularly well suited in determining how well geosynthetics would perform under stabilization of bases where transfer of stresses from the soil to the geosynthetic is expected along with resistance to those transferred stresses (high stiffness).

4 RESULTS

The performance of the various pavement sections is measured in terms of rutting. Rutting is measured from the post-trafficking surface deformation profiles, after correcting for pre-trafficking surface, as the maximum depth from the top of the heave next to the wheel path to the path of the trough under the wheel path as shown in Figure 5. These rut measurements were taken periodically after a pre-determined number of wheel passes. Figure 6 shows the rut measurements taken till failure of all five pavement sections with and without geogrid stabilization.

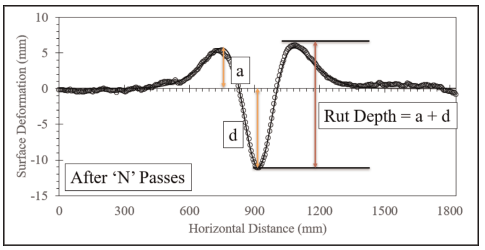

Figure 5. Typical rutting profile with 360 sample points from the laser profilometer.

4.1 *Traffic benefit ratio*

The improvement in pavement performance due to the stabilization of the base course can be quantified using the traffic benefit ratios (TBRs) obtained by comparing the rutting in the geogrid stabilized sections (GG1 to GG4) to that in the control section. This is possible because the only difference between the four geogrid stabilized sections and the control is the presence of geogrid. Thus, TBRs of each stabilized section is a direct measure of the improvement due to the corresponding geogrid.

For the purposes of this study, TBR due to geogrid stabilization may be defined as the ratio of the number of load repetitions to failure in the stabilized section to that in the control section, given identical pavement structure with the exception of the geogrid. From Figure 6, the number of wheel passes to various levels of rut are determined and their TBR is determined as follows.

$$TBR_{RD} = \frac{N_{GSS}}{N_{Control}} \tag{2}$$

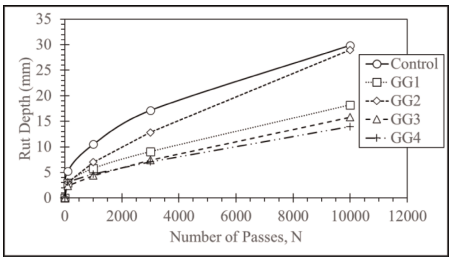

Figure 6. Progression of rutting with trafficking on all test sections.

where TBR_{RD} = Traffic Benefit Ratio at failure defined as rut = RD; N_{GSS} = Number of

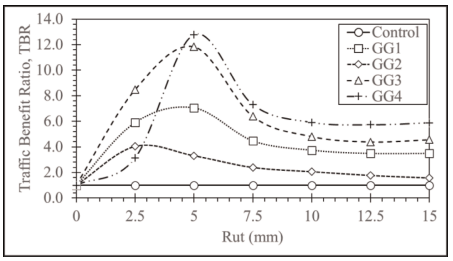

Figure 7. TBR as a function of rut for geogrid stabilized sections.

wheel passes to failure rut, RD, in geogrid stabilized section; and $N_{Control}$ = Number of wheel passes to failure rut, RD, in control section.

Thus, TBR for the various stabilized sections can be expressed as a function of the rut depth as shown in Figure 7. The TBR starts at 1.0 for very small values of rutting, increases rapidly to a maximum in the 2.5 mm to 5 mm rut range, decreases and asymptotes to a constant around 10 mm to 15 mm rut depth. This is likely due to the high relative density (85%) of the base layer within which the geogrid is placed. As the pavement surface is trafficked, the dense base layer begins dilating in the control section. But in geogrid stabilized sections, the dilatancy is reduced (Chen *et al.* 2018; Sweta & Hussaini 2018), resulting in increased TBR. As the deformations increase, the base material reaches the critical state, thus benefits from geogrid reduces and asymptotes to a constant value of TBR.

4.2 *Soil-geosynthetic composite stiffness and TBR*

Figure 8 compares the traffic benefit ratio obtained at critical state for each geogrid stabilized section with the soil-geosynthetic composite stiffness obtained from SGI tests between

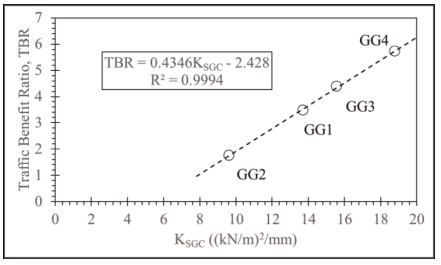

Figure 8. Traffic Benefit Ratio Vs. K_{SGC}.

the same geogrid and base material. Each circle represents the (TBR, K_{SGC}) pair of the particular geogrid. The dashed line is the linear regression line through the datapoint. It can be seen that the TBR of any stabilized section is linearly correlated with the K_{SGC} of the base course-geogrid composite used in the stabilized section. The high degree of linear correlation ($R^2 = 0.9994$) between TBR and K_{SGC} values shows that K_{SGC} is a direct measure of the improvement to pavement rutting performance due to the inclusion of the geogrid and is thus a strong justification for the use of K_{SGC} as a critical parameter in the selection of geogrids to be used as for base stabilization.

5 CONCLUSIONS

Reduced-scale accelerated pavement tests and soil-geosynthetic interaction tests were conducted with AASHTO#8 base material and four different types of geogrids. The K_{SGC} of the base material-geogrid composite for each geogrid was determined from the SGI tests and found to be over a range from 9 $(kN/m)^2/mm$ to 20 $(kN/m)^2/mm$. The traffic performance enhancement facilitated by the inclusion of the geogrid was evaluated by comparing it to a control section without geogrid stabilization as Traffic Benefit Ratio. It was found that traffic benefit ratio due to stabilization by any geogrid is a function of the failure rut depth. The TBR was found to increase with increasing failure rut depth up to a certain rut value and then decrease to an asymptotic value. This interesting behavior of stabilized sections is attributed to the dilation of the base material and the varying levels of reduction in dilatancy facilitated by the stabilizing geogrid.

It is also found that the asymptotic TBR of the stabilized sections differs by the type of geogrid used and is highly linearly correlated to the base material-geogrid composite stiffness determined from the SGI tests. Thus, K_{SGC} can be used to predict the performance of geogrid stabilized base layers in flexible pavements and therefore be used in the selection of geogrids for the application of stabilization.

REFERENCES

AASHTO R50. 2009. Standard Practice for Geosynthetic Reinforcement of the Aggregate Base Course of Flexible Pavement Structures. *American Association of State Highway and Transportation Officials*, Washington, D.C.

Archer S. & Wayne M. H. 2012. "Relevancy of Material Properties in Predicting the Performance of Geogrid-Stabilized Roadway." *Proc. of the Conference GeoFrontiers, Advances in Geotechnical Engineering*, ASCE, Oakland, California, pp.1320–1329

Chen, X., Jia, Y. and Zhang, J., 2018. Stress-strain Response and Dilation of Geogrid-reinforced Coarse-grained Soils in Large-scale Direct Shear Tests. *Geotechnical Testing Journal*, 41(3), pp.601–610.

Christopher, B. R., Cuelho, E. V., & Perknis, S. W. 2008. Development of Geogrid Junction Strength Requirements for Reinforced Roadway Base Design. *In Proceedings of GeoAmericas* 2008 Conference, Cancun, Mexico (pp. 1003–1012).

Epps Martin, A., Walubita, L.F., Hugo, F. and Bangera, N.U., 2003. Pavement Response and Rutting for Full-scale and Scaled APT. *Journal of Transportation Engineering*, 129(4), pp.451–461.

Roodi, G.H., & Zornberg, J.G. 2017. "Stiffness of Soil-geosynthetic Composite under Small Displacements. II: Experimental Evaluation." *Journal of Geotechnical and Geoenvironmental Engineering, ASCE*, Vol. 143, No. 10, October.

Sweta, K. and Hussaini, S.K.K., 2019. Behavior Evaluation of Geogrid-reinforced Ballast-subballast Interface Under Shear Condition. *Geotextiles and Geomembranes*, 47(1), pp.23–31.

TxDOT SS3239. 2004. Special Specification for Thin Overlay Mix (TOM). TxDOT

Zornberg, J.G., Roodi, G.H., & Gupta, R. 2017. "Stiffness of Soil-geosynthetic Composite under Small Displacements: I. Model Development." *Journal of Geotechnical and Geoenvironmental Engineering, ASCE*, Vol. 143, No. 10, October.